Behavior-Dependent Corticocortical Contributions to Imagined Grasping: A BCI-Triggered TMS Study

Houmin Wang, Huixian Zheng, Hanrui Wu, and Jinyi Long

***Abstract*— Previous studies have indicated that corticocortical neural mechanisms differ during various grasping behaviors. However, the literature rarely considers corticocortical contributions to various imagined grasping behaviors. To address this question, we examine their mechanisms by transcranial magnetic stimulation (TMS) triggered when detecting event-related desynchronization during right-hand grasping behavior imagination through a brain-computer interface (BCI) system. Based on the BCI system, we designed two experiments. In Experiment 1, we explored differences in motor evoked potentials (MEPs) between power grip and resting conditions. In Experiment 2, we used the three TMS coil orientations (lateral-medial (LM), posterior-anterior (PA), and anterior-posterior (AP) directions) over the primary motor cortex to elicit MEPs during imagined index finger abduction, precision grip, and power grip. We found that larger MEP amplitudes and shorter latencies were obtained in imagined power grip than in resting. We also detected lower MEP amplitudes during imagined power grip, while MEP amplitudes remained similar across imagined precision grip and index finger abduction in each TMS coil orientation. Differences in AP-LM latency were longer when subjects imagined a power grip compared with precision grip and index finger abduction. Based on our results, higher cortical excitability may be achieved when humans imagine precision grip and index finger abduction. Our results suggests that higher cortical excitability may be achieved when humans imagine precision grip and index finger abduction. We also propose that preferential recruitment of late synaptic inputs to corticospinal neurons may occur when humans imagine a power grip.**

***Index Terms*— Brain-computer interface (BCI), motor imagery, event-related desynchronization (ERD), I-waves, transcranial magnetic stimulation (TMS).**

I. Introduction

THE human mind is able to mentally simulate actions without actually performing them, which is also known as motor imagery. This remarkable ability has been elucidated through impressive contributions from experimental research. Evidence has shown the equivalence between actual and motor imagery tasks. For example, Decety et al. revealed that motor imagery can affects the physiological variables to the same proportionate degree as imagined efforts, similar to real movements [1]. Martine et al. proposed an experiment based on transcranial magnetic stimulation (TMS) at various interstimulus intervals (ITIs) to assess the excitability of fast and slow motor pathways in motor imagery contraction, executed contractions, and rest, and the results indicated that mental contractions and real contractions activate different corticospinal projections similarly [2]. In a previous study [3], Iacono et al. showed that continuous motor imagery training (back squat and bench press exercises) maintained and improved the physical performance of professional basketball athletes during detraining. Otherwise, experimental research in humans showed that imagined and real self-touch share the same recruitment of the forward models to predict the sensory consequences [4]. Consistently, motor imagery and motor execution activate the same frontal motor areas and parietal areas that overlap with the brain network [5], [6], [7]. The aforementioned evidence supports the hypothesis that motor imagery and executed movements are functionally equivalent [6], [8]. The study of motor imagery is fundamental not only for a basic understanding of brain mechanisms but also for promoting the development of applications in related fields [4]. Specifically, a study in humans has shown that later synaptic inputs are recruited to corticospinal neurons during real power grip induced by a single transcranial magnetic stimulation (TMS) coil oriented over the hand area of the primary motor cortex (M1) [9]. However, limited information exists on corticocortical contributions to imagined grasping.

Manuscript received 28 July 2022; revised 23 November 2022; accepted 4 December 2022. Date of publication 12 December 2022; date of current version 1 February 2023. This work was supported in part by the National Natural Science Foundation of China under Grant 62276115, in part by the Outstanding Youth Project of Guangdong Natural Science Foundation of China under Grant 2021B1515020076, in part by the Guangdong Provincial Key Laboratory of Traditional Chinese Medicine Informatization under Grant 2021B1212040007, and in part by the Fundamental Research Funds for Central Universities. The work of Hanrui Wu was supported in part by the National Natural Science Foundation of China under Grant 62206111, in part by the China Postdoctoral Science Foundation under Grant 2022M721343, and in part by the Fundamental Research Funds for Central Universities under Grant 21622326. *(Corresponding author: Jinyi Long.)*

This work involved human subjects or animals in its research. Approval of all ethical and experimental procedures and protocols was granted by The First Affiliated Hospital of Jinan University under Application No. KY-2020-036.

Houmin Wang, Huixian Zheng, and Hanrui Wu are with the College of Information Science and Technology, Jinan University, Guangzhou 510632, China.

Jinyi Long is with the College of Information Science and Technology, Jinan University, Guangzhou 510632, China, also with the Pazhou Laboratory, Guangzhou 510335, China, and also with the Guangdong Key Laboratory of Traditional Chinese Medicine Information Technology, Guangzhou 510632, China (e-mail: jinyil@jnu.edu.cn).

Digital Object Identifier 10.1109/TNSRE.2022.3227511

This work is licensed under a Creative Commons Attribution 4.0 License. For more information, see https://creativecommons.org/licenses/by/4.0/

Brain-computer interface (BCI) systems have been widely employed as tools to study motor imagery due to their effectiveness in linking brain activity with machine control. Event-related desynchronization (ERD) is considered to reflect the decrease in sensorimotor area oscillations which is recorded with electroencephalography (EEG) [10]. Many BCI paradigms use ERD as an online biomarker to explore motor cortical activity in motor imagery or in real movement [10], [11]. In a previous study [10], Takemi et al. proposed an ERD-based BCI experiment to identify agonist muscles that selectively disinhibit corticospinal output in imagined wrist movements with right hands. In addition, a motor imagery-based BCI control system has been adopted to explore corticospinal excitability [12]. These studies [10], [13], [14], represent considerable efforts to reveal the relationship between ERD and corticospinal excitability in motor imagery. Physiological studies further applied ERD as a biomarker to trigger TMS in an online BCI system. For instance, in a published study [15], Grigorev et al. showed that vibrotactile feedback was useful to increase corticospinal excitability in hand muscles during motor imagery with an ERD-based BCI system. Moreover, Dietz et al. proposed an ERD-based brain-machine interface to work effectively in the clinical recovery of functional movements [16]. Consistent with these studies, the physiological characteristics of ERD have been used as EEG markers in an online BCI system in the last few decades. These articles verified the effectiveness of ERD-based TMS BCI systems to investigate corticospinal contributions to grasp imagery.

Currently, studies examining the behaviors of different sets of cortical interneuronal circuits have received increasing attention [17], [18], [19]. For example, Gabrielle et al. performed biological research and showed that cortical interneuron presynaptic circuits exhibit area-specific in organization and development of their afferent connectivity during development [20]. Additionally, Mathieu et al. conducted cytology experiments and showed that the preoptic area gives a rise to neuroglia from cortical interneurons [18]. In particular, in a previous study [9], Monica et al. investigated the involvement of various sets of cortical interneuronal circuits during distinct hand grasping movements and found that later synaptic inputs to corticospinal neurons may be recruited when humans perform a power grip. However, the involvement of different sets of cortical interneuronal circuits are involved in various hand motor imaginations, particularly in hand grasping imagery, remains an open issue.

Motivated by the aforementioned discussions, we hypothesize that corticocortical contributions to grasping imagery may differ. We proposed employing different TMS coil orientations in an ERD-based real-time BCI system to verify this hypothesis. According to previous research [10], we set the ERD to 15% (high-level ERD) as the trigger condition for TMS. Specifically, we used the high-level ERD as the trigger condition for TMS to ensure that each motor imagery was effective. We performed two experiments in this study. Experiment 1 aimed to explore the difference in motor evoked potentials (MEPs), e.g., MEP amplitude and latency, between the imagined power grip and resting conditions. Subsequently, we designed Experiment 2, which focuses on 3 different hand grip imaginations, i.e., index finger abduction, precision grip, and power grip. Inspired by a previous study [19], we employed three direction TMS coil orientations, i.e., latero-medial (LM), posterior-anterior (PA), and anterior-posterior (AP), to investigate the different cortical structures that were activated during the three grasping imaginations. Additionally, we adjusted the MEP amplitudes to approximately 0.8 mV in Experiments 1 and 2 to eliminate the effects of different MEP sizes on MEP latency. Here, we highlight our contributions as follows:

- We applied an ERD-based motor imagery BCI system to investigate the corticocortical contributions to grasping imagination.
- Higher cortical excitability may be achieved when humans imagine precision grip and index finger abduction.
- Late synaptic input to corticospinal neurons may be activated when humans imagine a power grip.

The remainder of the paper is organized as described below. We introduce our methods in Section II. Then, we discuss the experimental results in Section III. Section V presents the conclusions of the study.

II. Methods

A. Subjects

Twenty-three volunteers were recruited from Jinan University through social media and e-mail. During the process of the experiment, three of them were unable to focus on performing imaginary motor tasks, and two of them reported that they were uncomfortable with the TMS; hence, five volunteers were excluded. Consequently, eighteen naive volunteers, i.e., eleven men and seven women aged 22.3±2.71 years, participated in this study. All subjects were right-handed according to self-report, with no mental or other illnesses. Subjects were required to complete a written consent form before the experiments. In addition, they were informed that their personal identifying data will not be collected other than general demographics if applicable, such as sex, general characteristics, and age range. Our experimental procedures were approved by the local ethics committee at Jinan University and were conducted in accordance with the guidelines established in the Declaration of Helsinki.

Two experiments were performed, one in which subjects only performed one hand motor imagery task (power grip) and one in which subjects imagined performing three hand grasping tasks (index finger abduction, precision grip and power grip). The eighteen subjects were randomly assigned to one of these experiments. Therefore, nine subjects (three women) participated in Experiment 1, and nine subjects (four women) participated in Experiment 2.

B. Experimental Paradigm and Tasks

A brief schematic of the experimental protocol visual representation is shown in Fig. 1A. The experiments were conducted in a quiet and silent room. Generally, two hours were required to complete all trials in each experiment and

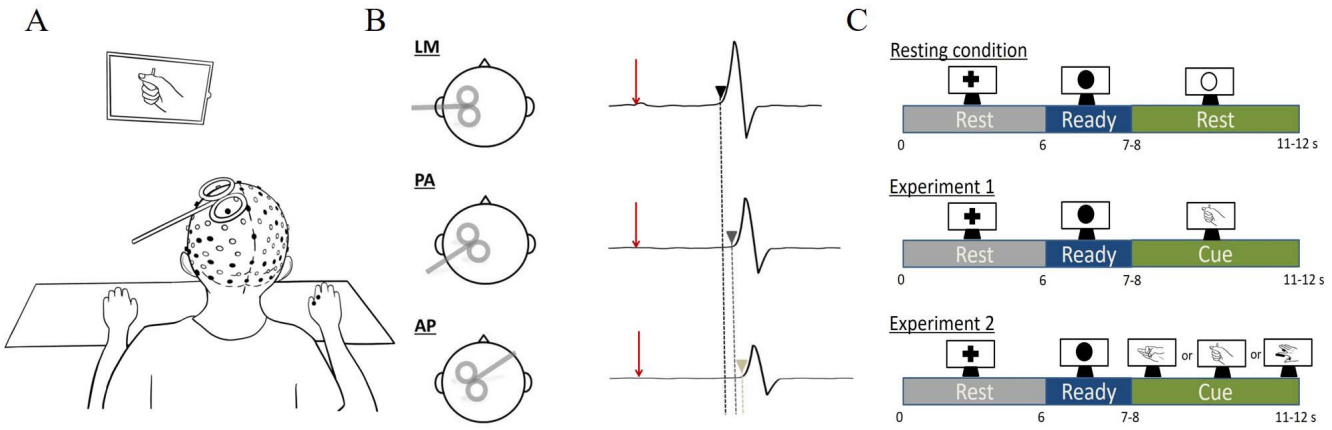

Fig. 1. (A) Overview of the experimental protocol. Subjects received task images from a monitor. MEP is measured via FDI muscle. (B) Representative traces show motor evoked potentials (MEPs) in MI task with 3 coil currents, i.e., LM, PA, and AP. The latencies of the red arrow indicates the moment when the TMS appears. (C) The whole experiment setup of resting condition experiment 1 and experiment 2.

fit the conductive cap. The subjects sat in a comfortable customized armchair with their hands placed palm side down on a table. A 24-inch monitor was placed 1.2 meters in front of the armchair to guide subjects in performing the motor imagery tasks. E-prime 3.0 (designed by PST, US) controlled the experimental setup.

Fig. 1B represents a schematic sketch of the TMS coil orientations. Representative curves show the examples of motor evoked potentials (MEPs) during imagined power grip with the coil currents in LM, PA, and AP. The red arrow indicates the moment when the TMS was applied, and the dotted lines illustrate the MEP onset point.

As shown in Fig. 1C, our experimental setup consisted of resting conditions, Experiment 1, and Experiment 2. The resting condition served as the control experiment. All eighteen subjects were asked to participate in the resting condition. To ensure subjects can do the motor imagery tasks properly. Before the experiments, we asked the subjects to perform 4s of sustained power grip, index finger abduction, or precision grip with their right hand at maximal voluntary contraction (MVC) strength 5 times to ensure that they were able to perform the imagery tasks properly. Each experiment was conducted on the same day with the same physiological signal acquisition settings. The resting conditions were always conducted first to eliminate the fatigue of motor imagery tasks. Before the experiments, the main experimenter introduced the experimental procedure and tasks to each subject. During each experiment, the other experimenter monitored the electromyographic (EMG) signal curves in front of a monitor to ensure that the subjects' hands were relaxed [20], [21], [22], [23].

1) Protocol for Resting Conditions: In each trial of a resting condition, a fixation cross was displayed for 6 s before the presentation of a black circle for 1-2 s, then a white circle appeared for 4 s. The ready duration was set to 1-2 s to eliminate EEG signal pollution caused by the neural plasticity in the same time scheme. Subjects were asked to rest when the fixation cross and white circle appeared, and prepare when the black circle appeared. Each TMS orientation consisted of one block containing 30 trials, and 80% of the trials triggered the TMS in random order.

2) Protocol for Experiment 1: Subjects were told to rest when the fixation cross appeared for 6 s and prepare when the black circle appeared for 1-2 s. After the black circle appeared, a power grip cue image was shown on the screen for 4 s. During the appearance of the image, the subjects were required to imagine the sustained power grip with their right hands. Similar to the protocol for resting conditions, each TMS orientation consisted of a block with 30 trials.

3) Protocol for Experiment 2: In Experiment 2, the flow time was the same as in Experiment 1 for the ready and resting sessions. After the white circle appeared, imperative cues consisting of index finger abduction, precision grip, and power grip were presented on the screen. Each TMS orientation contained three blocks, and each cue image in one block appeared ten times randomly.

C. EEG Measurement and Analyses

EEG data were acquired from 9 scalp sites (extended 10-20 system) placed at C3 and 30 mm anterior, posterior, medial, and lateral to C3 to cover the sensorimotor hand area using a cap with active Ag/AgCl electrodes (quickcap64). The EEG data were re-referenced by the 8 neighboring electrodes. The ground electrode was placed between the Fpz channel and Fz channel. The impedance of all electrodes was maintained below 5 kΩ throughout the experiments. The reference electrodes were placed on the bilateral mastoids. The sampling rate of the EEG signal was 1 kHz. The bandpass filtering range was 0.5–30 Hz with a 50-Hz notch filter. The 8-20 frequency band is known as the majority of the ERD response range and is widely used in ERD-based BCI systems [24]. Therefore, we chose this frequency band for ERD calculations. A Neuroscan Synamps2 amplifier was used to amplify the EEG signal. The sampling rate of the EEG signal was 1 kHz. We used MATLAB 2018a (The Mathworks, Natick, MA) for the online EEG data calculation. EEG data were acquired

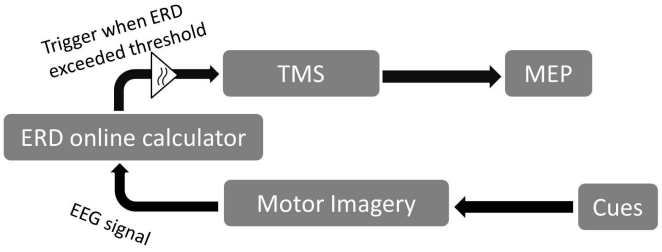

Fig. 2. EEG online process diagram in BCI online system. EEG electrodes are placed around the right-hand sensorimotor. EEG signals are calculated by the ERD online calculator. The calculated data was sent to an analog-to-digital (A/D) converter (CED Micro 1401, Cambridge Electronic Design, UK). When the ERD exceed the threshold (15% ERD), a single-pulse transcranial magnetic stimulation (TMS) is applied to the M1 area. The MEP is obtained from the target muscle (FDI).

using Curry 8 software. The marks from the presentation software (E-Prime 3.0) were sent to Curry 8.

The acquired EEG data were sent to a MATLAB script to perform the online ERD calculation. Once the ERD exceeded the predetermined threshold (15%), TMS was triggered. The real-time ERD calculation procedure involved (1) reading EEG data from C3 and re-referencing by the 8 neighboring electrodes, (2) estimating the power spectrum density within the frequency band of 8-20 Hz in each 2000 ms Hanning windowed with fast Fourier transformation (FFT), and (3) calculating the ERD at each segment with a 100 ms time resolution and a 1 Hz frequency.

When the 4 s cue image appeared in Experiment 1 and Experiment 2. The ERD (%) was rescaled as a percentage of baseline every 100 ms within a 2 s length window using Formula 1. The length of the 2 s window covered the latest 2 s of EEG data. As a result, we calculated the ERD (%) as follows:

$$\mathrm{ERD}(\%) = \frac{\bar{R}(f) - A(t, f)}{\bar{R}(f)} \times 100\%, \tag{1}$$

where $A(t, f)$ indicates the PSD (power spectrum density) at time-frequency point (t, f). $\bar{R}(f)$ is the FFT mean power spectrum in the baseline period (3 s time interval in the resting period in Experiment 1 and Experiment 2).

An overview of the EEG online process diagram is presented in Fig. 2. EEG electrodes were placed around the left sensorimotor area. The ERD online calculator transformed the EEG signal to the percentage as the baseline. The calculated data were sent to an analog-to-digital (A/D) converter (CED Micro 1401, Cambridge Electronic Design, UK). When the ERD exceeded the threshold, single-pulse TMS was applied to the primary motor cortex (M1) area. The MEP was obtained from the target muscle.

D. Motor Evoked Potentials

The resting motor threshold (RMT) was determined at the lowest stimulus intensity eliciting MEPs in the target muscle (FDI) with a $> 50\ \mu$V peak-to-peak amplitude in a minimum of 5 out of 10 consecutive trials [26]. Higher stimulus intensities are required in the LM currents to stimulate corticospinal neurons directly (D-wave) [23]. Therefore, we set the stimulus intensity in the LM direction to 150% RMT and set the stimulus intensity in the PA and AP directions to 110% RMT. We also compared MEP amplitudes between tasks and resting conditions in Experiment 1 and Experiment 2. MEP amplitudes and latencies were averaged from 20 trials in each coil current and each task. MEP onset latency was calculated for individual trials in each subject and condition. The MEP latency was set as the point at where 2 standard deviations above the mean rectified EMG signal was obtained in each trial (calculated 100 ms before the stimulus). We applied a script to calculate the MEP onset latencies in spike 2 as a method to avoid visual errors. We compared the MEP latencies in PA and AP currents with LM currents. PA-LM and AP-LM were used as measurements to quantify early and late I-wave recruitment. To eliminate the differences in MEP onset latencies were influenced by the MEP amplitudes. We conducted the control experiments by adjusting the MEP size to 0.8 ± 0.03 mV across tasks in Experiment 1 and Experiment 2.

E. EMG Recordings

Before each experiment, the main experimenter cleaned the subjects' right hands with alcohol wipes to avoid muscle signal noise caused by sweat and surface oil. Surface electromyographic (EMG) activity was recorded from the first dorsal interosseous (FDI) muscle by Ag-AgCl surface electrodes (10-mm diameter). The ground electrode was placed on the ulna near the wrist. The EMG signal is amplified and filtered (5–2,000 Hz) with a bioamplifier (Neurolog System, Digitimer, UK). An analog-to-digital converter (CED Micro 1401, Cambridge Electronic Design, UK) was applied to digitize EMG signals with a sampling rate at 5 kHz. The EMG signal is stored on a computer for offline analysis by using EMG acquisition software (Spike 2). The EMG signal was not only monitored by the experimenter but also using the offline analysis to discard background EMG activities more than $\pm$ 0.025 mV [10].

F. Transcranial Magnetic Stimulation

A figure-8 coil TMS stimulator (Magstim BiStim2; Magstim, Whiteland, UK) with a monophasic current waveform was used to activate MEP (motor evoked potentials). By changing the current flow through the MI area, a single pulse can activate different synaptic inputs to corticospinal neurons [9], [25]. Thus, the 3 coil orientations were applied across the hand area of M1 in the motor imagery task. The 3 coil orientations are specifically described below. 1). The coil was held at an angle of 90 degrees to the midline (LM current). 2). The coil was fixed at an angle of 45 degrees to the midline, and the handle pointed laterally and posteriorly (PA current). 3). The orientation of the coil was reversed around the intersection at 180 degrees to the PA current (AP current). During our experiment, all of the subjects' heads were maintained in a comfortable position. After each block, the subjects were allowed a five-minute break to adjust their bodies to an optimal position. The TMS hotspot was determined by PA currents, as previous research showed that currents did not affect the

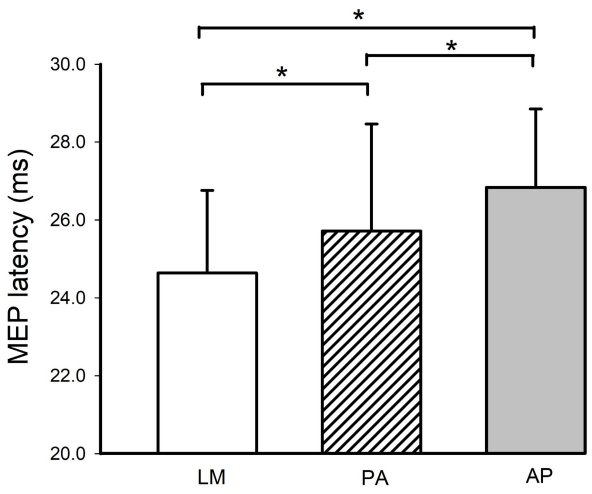

Fig. 3. MEP latencies in each coil orientation in resting condition. MEP latencies elicited by AP and PA currents were prolonged than LM. Note, MEP latencies were longer with AP than PA directed currents.* $P < 0.05$.

position of the hotspot [26]. The motor hotspot was marked with a marker pen on the scalp, which was placed on the head as the reference to rotate the coil [27]. The TMS coil was held by an experienced operator. The average number of missing trials is 7 ± 3 for the whole.

We confirmed that latencies of MEPs elicited by AP and PA directed currents were prolonged compared with LM currents for each participant to ensure that we conducted the TMS orientation paradigm (AP, PA, and LM) properly. Additionally, the MEP latencies were longer with AP compared with PA directed currents (Fig. 3). To avoid TMS introducing electronic noise to the EEG signal, we tried to prevent the coil from resting on the scalp in our experiment to ensure that the TMS coil did not introduce significant artifacts and electronic noise into the EEG data. Additionally, TMS stimulation has a very short duration (< 10 ms). In Fig.1C, a minimum of 7 seconds elapsed between each stimulus, and thus the TMS artifact could be easily trimmed. Our method is appropriate.

G. Statistical Analysis

We used the SPSS statistical software system (version 25.0) for data analysis. SigmaPlot (version 11.0) was used for data visualization and presentation. The Shapiro-Wilk test was used to test normal distribution. Mauchly's test was applied to ensure sphericity. The Greenhouse-Geisser correction statistic was applied when sphericity could not be assumed. In Experiment 1, we performed a two-way repeated-measures ANOVA analysis to determine the effect of conditions (resting condition and imagined power grip) and coil orientations (LM, PA, and AP) on MEP latency and MEP amplitude. In Experiment 2, we used two-way repeated-measures ANOVA to determine the effect of tasks (imagined index finger abduction, precision grip and power grip) and coil orientations (LM, PA, and AP) on MEP latencies and MEP amplitudes. Significant comparisons were assessed using Bonferroni post hoc tests. The significance level is considered at $P < 0.05$.

TABLE I
REPEATED MEASURES ANOVA ANALYSIS RESULTS IN EXPERIMENT 1

		Tasks	Coil orientations	Interaction
Experiment 1	Latency	$F_{1,8}$ = 6.82, P <0.05	$F_{1,8}$ = 9.15, P <0.05	$F_{1,8}$ = 5.26. P <0.05
	Amplitude	$F_{2,7}$ = 8.38, P <0.05	$F_{1,8}$ = 11.45, P <0.05	$F_{2,7}$ = 6.06, P <0.05
Experiment 1 (Adjusted)	Latency	$F_{1,8}$ = 5.77, P <0.05	$F_{2,7}$ = 5.81, P <0.05	$F_{1,8}$ = 6.73. P <0.05
	Amplitude	$F_{3,6}$= 1.18, P = 0.53	$F_{3,6}$ = 2.25, P = 0.33	$F_{2,7}$= 3.06, P = 0.24

TABLE II
MEP AMPLITUDE AND LATENCY RESULTS IN EXPERIMENT 1

		Power Grip	Rest	P - value
Experiment 1	MEP amplitude	1.1 ± 0.6 mV	0.8 ± 0.4 mV	P <0.05
	MEP latency	22.7 ± 1.9 ms	21.5 ± 1.8 ms	P <0.05
Experiment 1 (Adjusted)	MEP amplitude	0.8 ± 0.031 mV	0.8 ± 0.023 mV	P = 0.41
	MEP latency	21.3 ± 1.9 ms	22.4 ± 2.0 ms	P <0.05

III. RESULTS

In Experiment 1, the results showed that larger MEP amplitudes and shorter MEP latencies were obtained in imagined power grip compared with resting conditions. In Experiment 2, our results indicated lower MEP amplitudes during the imagined power grip, while the MEP amplitudes remain similar across imagined precision grip and index finger abduction in each TMS coil orientation. The AP-LM latency differences were longer when subjects imagined a power grip than when they imagined a precision grip and index finger abduction.

A. Experiment 1

Fig. 4A illustrates the mean values of the MEP amplitudes recorded in Experiment 1. Repeated measures ANOVA showed a significant effect of tasks, coil orientations and in their interaction on MEP amplitudes (TABLE I). Post hoc analysis revealed that the amplitudes of MEPs were higher for each coil orientation when subjects imagined power grip compared with the resting condition (TABLE II; Fig. 4A). Similar ANOVA analysis showed a significant effect of tasks, coil orientations and in their interaction on MEP latency (TABLE I). Post hoc analysis revealed that the MEP onset latencies were significantly longer in resting condition (TABLE II; Fig.4B).

In the control experiment, we matched the MEP amplitudes at 0.8 ± 0.03 mV in the resting condition and motor imagery condition (TABLE II; Fig. 5A). Here, a two-way repeated-measures ANOVA showed a significant effect of tasks, coil orientations and in their interaction on MEP latency (TABLE I). Post hoc tests showed that the MEP latency in the imagined power grip condition was significantly shorter than that in the resting condition when the MEPs were adjusted (TABLE II. Hence, the result of MEP latency was similar with and without MEP adjustments (see Fig. 5B).

B. Experiment 2

Fig. 6A shows EMG curves from a representative subject that were recorded from the FDI muscle during imagined index finger abduction (black), precision grip (gray), and power grip

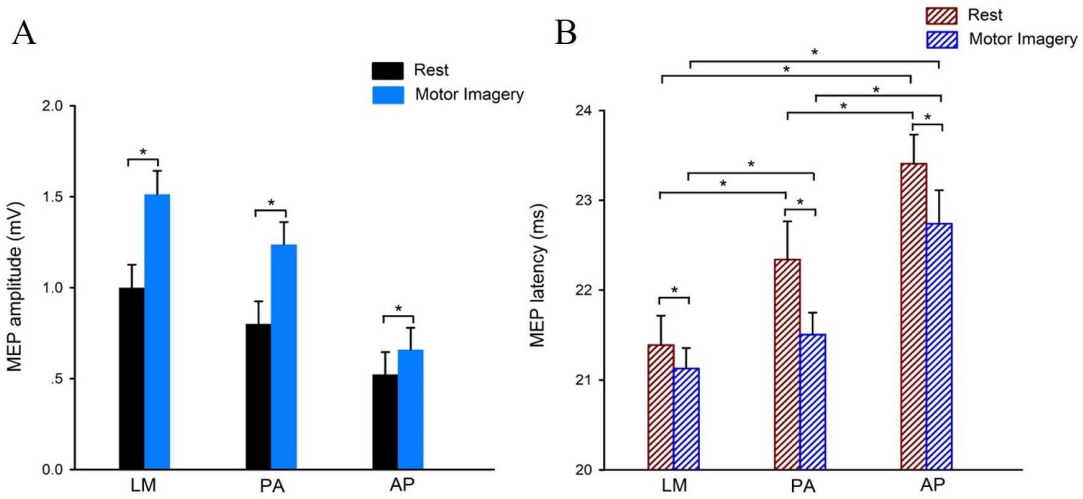

Fig. 4. (A) MEP amplitudes. Group data (n = 9) shows the MEP amplitudes during the resting condition (black bar) and motor imagery condition (blue bar) in each TMS coil orientation. Note that MEP amplitudes during imagined power grip is higher compared with resting condition. (B) MEP latency. Group data (n = 9) shows MEP latencies during resting condition (red fine pattern bar) and motor imagery condition (blue fine pattern bar) in each TMS coil orientation. Notably, MEP latencies in the imagined power grip condition were shorter than resting condition. Error bars indicate SEs. $^{*}P < 0.05$.

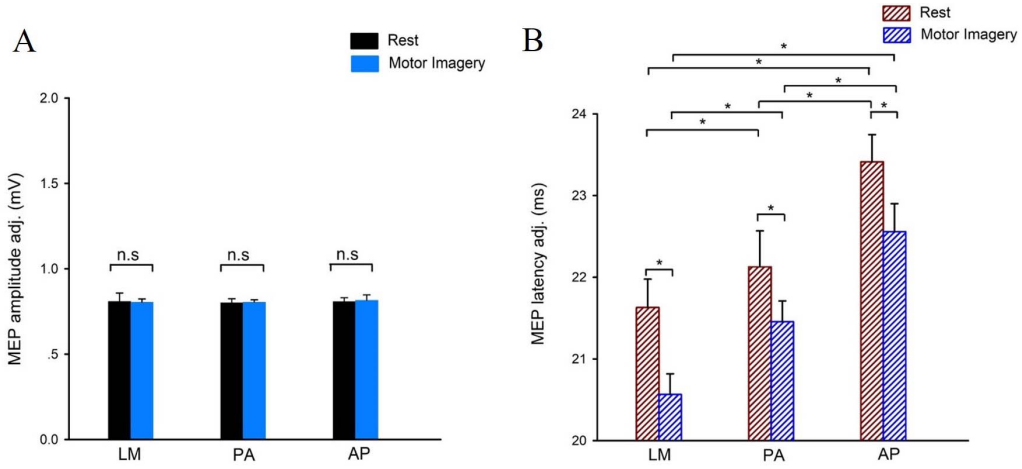

Fig. 5. (A) Adjusted MEP amplitudes. Group data (n = 9) shows MEP amplitudes during the resting condition (black bar) and motor imagery condition (blue bar)in each TMS coil orientation in the control experiment. $^{n.s}P = 0.41$. (B) MEP latency. Group data (n = 9) indicates the MEP latencies in resting condition (red fine pattern bar) and imagined (blue fine pattern bar) conditions in the control experiment. Note that MEP latencies in the imagined power grip condition were shorter than the resting condition. Error bars indicate SEs. $^{*}P < 0.05$.

(dotted gray). MEP traces are elicited with the coil oriented in LM (left), PA (middle), and AP (right) directions. We observed that the MEP onset latency differences were prolonged during imagined power grip compared with imagined precision grip and imagined index finger abduction. Note the similarities in MEP latency at each coil orientation during imagined index finger abduction and imagined precision grip. TABLE V shows that the MEP latency in the imagined power grip condition was significantly longer than that in the index finger abduction and precision grip conditions, with a significant differences observed between rest and imagined grasping behaviors ($^{*}P < 0.05$, Fig. 6B).

We compared the MEP latency differences between the three motor imagery tasks. Repeated measures ANOVA showed a significant effect of latency differences, tasks and in their interaction on I-wave recruitment (TABLE III). Post hoc analysis revealed that PA-LM MEP latency differences were similar across MI tasks ($P = 0.22$; TABLE IV; Fig. 7). Note that the AP-LM latency differences during imagined power grip are significantly longer than in imagined precision grip and imagined index finger abduction (TABLE IV; Fig. 7). Notably, AP-LM MEP latency differences in imagined index

TABLE III
REPEATED MEASURES ANOVA ANALYSIS RESULTS IN EXPERIMENT 2

		Tasks	Latency differences	Interaction
Experiment 2	Latency	$F_{1,8} = 6.45$, P <0.05	$F_{2,7} = 2.78$, P <0.05	$F_{2,7} = 8.76$, P <0.05
	Amplitude	$F_{1,8} = 6.03$, P <0.05	$F_{1,8} = 17.04$, P <0.05	$F_{2,7} = 8.06$, P <0.05
Experiment 2 (Adjusted)	Latency	$F_{2,7} = 13.12$, P <0.05	$F_{1,8} = 9.38$, P <0.05	$F_{2,7} = 0.13$, P = 0.91
	Amplitude	$F_{3,6} = 1.08$, P = 0.59	$F_{2,7} = 1.12$, P = 0.38	$F_{3,6} = 0.93$, P = 0.68

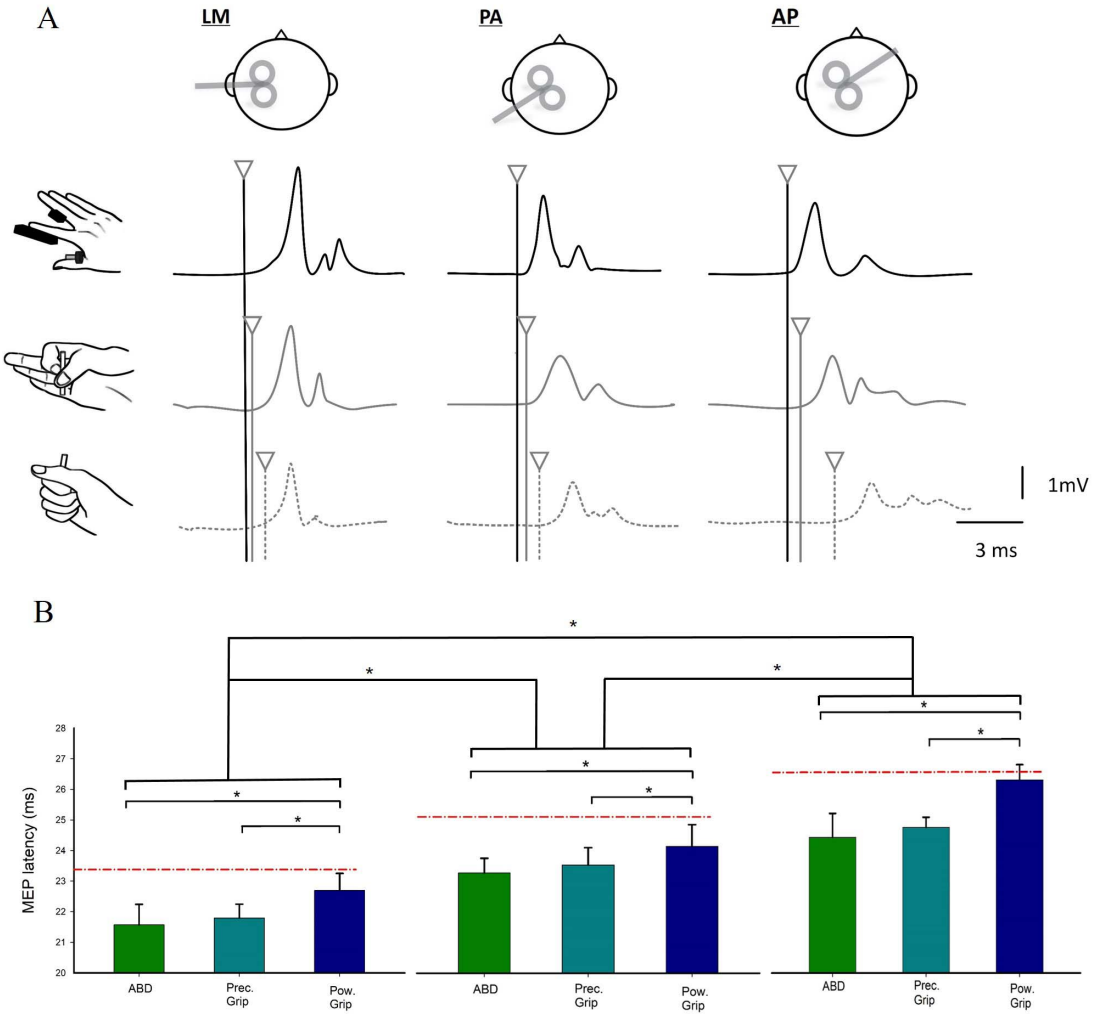

Fig. 6. (A) The representative MEP onset latency elicited in the FDI muscle for a representative subject during imagined index finger abduction (black line), imagined precision grip (gray line) and imagined power grip (dotted gray line) with the TMS coil oriented in LM (left), PA (center) and AP (right) direction. The rectified MEP curves represent the average of 20 trials. (B) Group data (n = 9) shows MEP latency during imagined index finger abduction (green bars), precision grip (blue-green bars), power grip (blue bars), and rest conditions (red line) with the three coil orientations. Error bars indicate SEs. $^{*}P < 0.05$.

TABLE IV
MEP LATENCY DIFFERENCES RESULTS IN EXPERIMENT 2

		ABD	Precision Grip	Power Grip	Rest
Experiment 2	PA - LM	1.5 ± 0.5 ms	1.5 ± 0.3 ms	1.3 ± 0.5 ms	1.6 ± 0.6 ms
	AP - LM	2.5 ± 1.1 ms	2.5 ± 1.0 ms	3.0 ± 1.0 ms	2.5 ± 0.7 ms
Experiment 2 (Adjusted)	PA - LM	1.3 ± 0.5 ms	1.1 ± 0.4 ms	1.5 ± 0.6 ms	1.4 ± 0.5 ms
	AP - LM	2.1 ± 0.3 ms	1.8 ± 0.7 ms	3.0 ± 0.8 ms	2.5 ± 0.6 ms

TABLE V
MEP LATENCY AND AMPLITUDE RESULTS IN EXPERIMENT 2

		ABD	Precision Grip	Power Grip	Rest
Latency	LM	21.6 ± 0.6 ms	21.8 ± 0.4 ms	22.8 ± 0.3 ms	23.4 ± 0.5 ms
	PA	23.1 ± 0.3 ms	23.3 ± 0.4 ms	24.0 ± 0.5 ms	24.9 ± 0.4 ms
	AP	24.1 ± 0.7 ms	24.3 ± 0.3 ms	25.8 ± 0.4 ms	26 ± 0.6 ms
Amplitude	LM	2.2 ± 0.7 mV	2.1 ± 0.8 mV	1.7 ± 0.5 mV	1.4 ± 0.4 mV
	PA	1.8 ± 0.5 mV	1.7 ± 0.5 mV	1.5 ± 0.4 mV	1.2 ± 0.6 mV
	AP	1.2 ± 0.2 mV	1.3 ± 0.2 mV	1.0 ± 0.3 mV	0.8 ± 0.3 mV

finger abduction were not significantly different from the imagined precision grip (TABLE IV; $P = 0.409$).

We matched the MEP amplitudes to 0.8 ± 0.03 mV across tasks in each TMS coil orientation ($P = 0.58$; TABLE III; Fig. 7). Repeated measures ANOVA showed a significant effect of MEP latency differences but not in their interaction on MEP recruitment (TABLE III). Post hoc analysis revealed that PA-LM MEP latency differences were similar across MI tasks ($P = 0.69$; TABLE IV; Fig. 7). Here, we observed that the AP-LM latency differences in the imagined power grip were significantly longer than those in the imagined precision grip and imagined index finger abduction (TABLE IV; $P < 0.05$). The results revealed that the significant differences in MEP latency were not influenced by MEP size.

Fig. 8A shows a schematic of the TMS coil oriented in the LM (left), PA (middle) and AP (right) directions. Fig. 8B

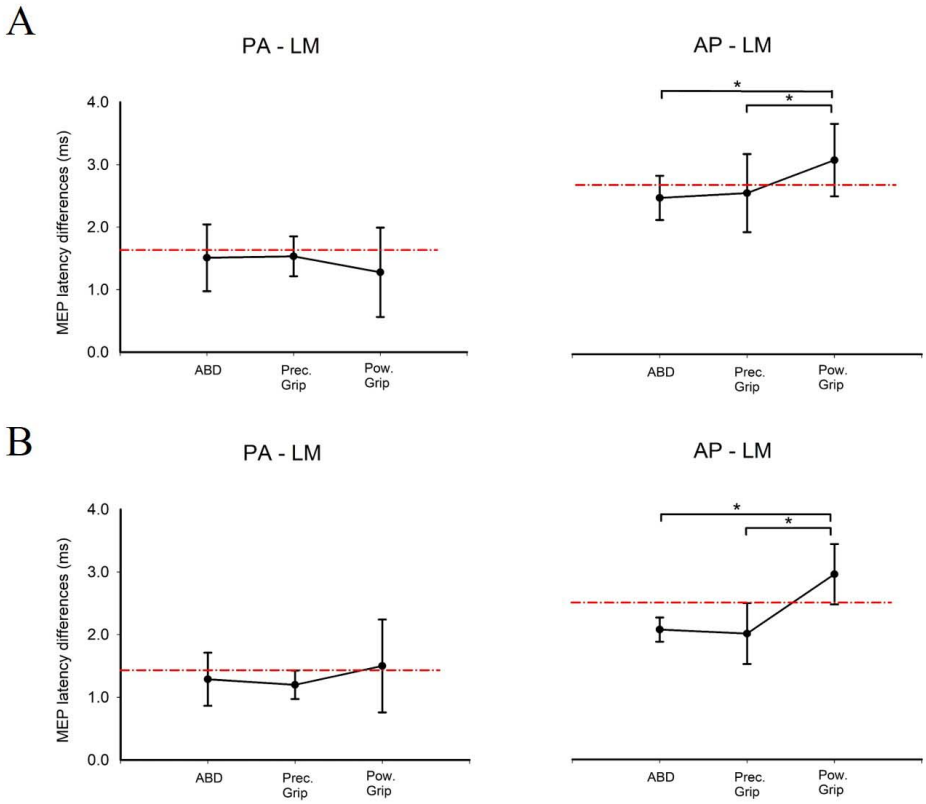

Fig. 7. MEP latency differences.(A) Group data (n = 9) shows the PA-LM and AP-LM MEP latency differences during imagined index finger abduction, imagined precision grip, imagined power grip, and rest condition (red dotted line) in Experiment 2. (B) Group data (n = 9) shows MEP latency differences during imagined grasping behaviors and rest conditions (red dotted line) in adjusted Experiment 2. Error bars indicate SEs. $^{*}P < 0.05$.

indicates the MEP elicited in the FDI muscle for a representative subject during the MI tasks and resting condition, index finger abduction (green line), precision grip (blue-green line), power grip (blue line) and resting condition (red dotted line). We compared the differences in MEP amplitudes among the three motor imagery tasks with resting condition. Repeated measures ANOVA showed a significant effect of tasks, coil orientations and in their interaction on MEP amplitudes (TABLE III). Post hoc tests revealed larger MEP amplitudes in imagined precision grip and index finger abduction than imagined power grip tasks($P < 0.05$), but no significant differences were observed between imagined index finger abduction and imagined precision grip ($P = 0.075$, Fig. 8C; TABLE V).

IV. Discussion

In this study, we tested corticocortical contributions to grasping imagination using a motor imagery-based BCI system. Our findings are summarized as bellow. First, significant increases in MEP amplitudes were observed the imagined power grip condition compared with the resting condition. This increase is consistent with the relationship between imagined and voluntary hand movements. Second, we found that corticospinal neurons may preferentially recruit later synaptic inputs when humans imagine a power grip. Third, our results reveal that higher cortical excitability may be achieved when humans imagine precision grip and imagined index finger abduction than when they imagine power grip. Our experimental results also provide strong evidence that supports the functional equivalence between motor executions and motor imagery.

A. ERD-Triggered TMS BCI System

ERD is commonly used as a control biomarker in BCIs [10]. For example, agonist muscle induced selective disinhibition of corticomotor representations in a motor imagery-based BCI system, as evidenced by the ERD of cortical activity [10]. Alternating TMS coil currents activate various intracortical circuits to corticospinal neurons [28]. Notably, no previous studies have applied different TMS coil orientations in motor imagery-based BCI systems.

Ian et al. tested the relationship between ERD strength and corticospinal excitability induced by an ERD-triggered TMS system during hand contraction [29]. ERD can be used as an online readouts of motor cortical activity in motor imagery and execution [30], [31], [32]. After reviewing previous studies, most did not ensure that the subjects effectively performed the motor imagery tasks by observation as they did in the actual tasks. Physiological research shows that BCI can fill the gap between motor imagery and motor execution [33]. In the current study, we designed an ERD-triggered TMS BCI system with LM, PA, and AP TMS currents to assess

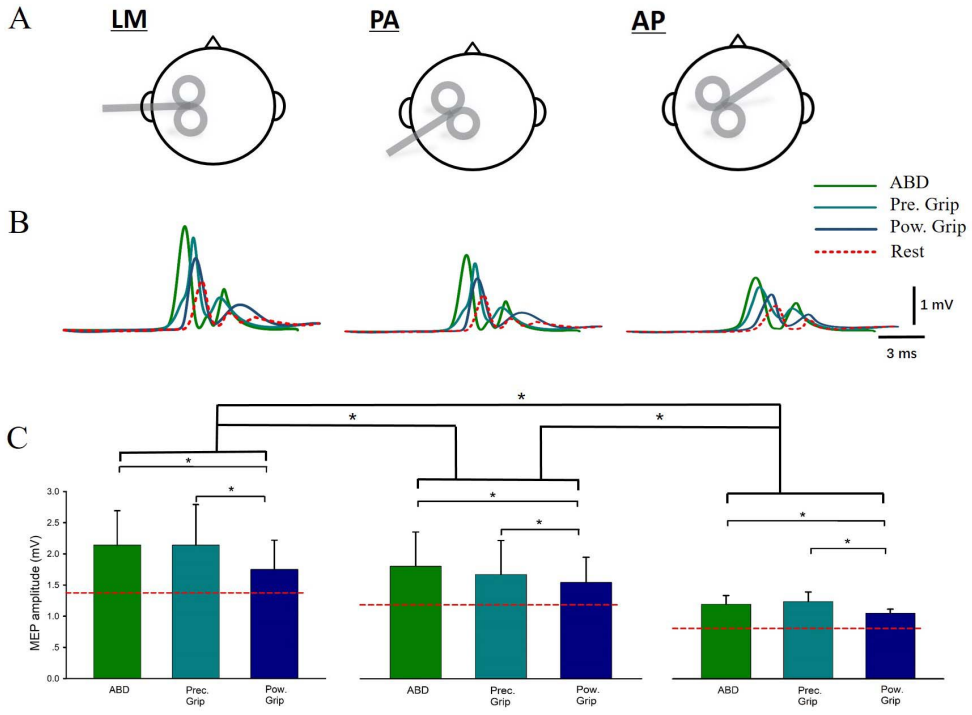

Fig. 8. (A) Represent the schematic in LM (left), PA (middle), and AP (right) TMS coil orientations. (B) Sample MEP curves for a representative subject during three motor imagery tasks and resting condition. Imagined index finger abduction (green line), imagined precision grip (blue-green line), imagined power grip (blue line) and resting condition (red dotted line). The rectified MEP curves represent the average of 20 trials. (C) Group data (n = 9) shows MEP latency during imagined index finger abduction (green bars), precision grip (blue-green bars), power grip (blue bars), and rest conditions (red line) with the three coil orientations. Note that the higher MEP amplitudes were obtained during imagined index finger abduction and imagined precision grip compared with imagined power grip. Error bars indicate SEs. $^{*}P < 0.05$.

the synaptic input during imagined index finger abduction, imagined precision grip, and imagined power grip. In contrast to the study by Takemi et al. [10], we do not have visual feedback of ERD strength in the experimental setup. A previous study documented that visual feedback may not affect corticospinal excitability [29]. We determined the ERD strength to be 15% in our study. However, corticospinal excitability may be modulated by different ERD strengths [29]. We cannot exclude the possibility that other ERD strengths may affect our results. Although we believe this limitation has not affected the primary outcome of the present study, future work could explore the relationship between ERD strength and corticocortical contributions to imagined grasping.

B. Functional Equivalence Between Motor Imagery and Motor Execution

Functional equivalence has long been theorized in previous studies. For example, a behavioral study showed that the same brain area was activated in motor imagery and motor execution [34]. Konstantina et al. showed that imagined self-touch produces somatosensory attenuation similar to the executed movements [35]. The main conclusion in the current study is that imagined power grip recruited later synaptic inputs similar to executed hand grasping does. Our findings provide strong evidence of the functional equivalence between the imagination and execution of movements.

Our results are consistent with a previous study [36] showing that late synaptic inputs might be preferentially recruited when humans perform a power grip. Based on our results, we believe that imagining a grasp engages the same mechanism as executing the imagined action. This functional equivalence may be computationally less expensive than employing different mechanisms for motor imagery and motor execution.

C. Contributions of Synaptic Input in Imagined Grasping

Our results showed longer MEP latencies during imagined power grip than index finger abduction and precision grip. An essential question to address in the current study is whether our results are consistent with previous studies. Our results are consistent with a literature review indicating that the MEP latencies elicited by PA and AP orientation are around 1.5 and 3.0 ms longer than the LM current during executed hand movements [37]. These results are also compatible with the MEP latency differences between D- and I-waves recorded from the epidural space [38], [39]. The available findings suggests that PA and AP TMS coil orientations preferentially activate early I-waves and later I-waves, and it is thought that 2 different synaptic inputs to corticospinal neurons are presumed to be recruited by the two TMS coil orientations? [37], [39]. Hence, consistent with previous studies, our experiment enable us to investigate different synaptic inputs involved in imagined grasping using LM, PA, and AP TMS coil orientations.

Several studies have hypothesized that the changes in MEP latencies with different TMS coil orientations may contribute to neuroplasticity [40], [41], [42]. Our results provide evidence that the same approach to increasing neuroplasticity

may be used in motor imagery. In a similar agreement [36], we observed significant differences between AP-LM but not PA–LM MEP latency differences during imagined grasping, and the synaptic inputs elicited by AP currents were more responsive during imagined grasping.

D. Functional Consideration

What is the relationship between different characteristics of the motor imagery tasks and MEPs? Although a gap is noted between the functional relevance of MEP latency differences and motor imagery tasks, previous studies have shown that changes in MEP latencies induced by different coil currents might provide a strong evidence into the ability of neural plasticity [43], [44]. In our study, the results with a significant difference in AP-LM MEP latency are presumed to preferentially recruit later I-waves with TMS in subjects. Hamada et al. proposed that a longer AP-LM should be considered as a better ability to induce cortical plasticity [43]. Similarly, our results indicate significant AP-LM but not PA-LM MEP latency differences, suggesting that AP currents are more responsive to different task changes during imagined grasping manipulations.

Our experimental results show that higher corticospinal excitability during imagined precision grip and index finger abduction. The results are consistent with a previous electrophysiology study suggesting that more dexterous finger contraction recruits a significantly larger number of corticospinal neurons compared with imagined power grip [45]. Yahagi et al. indicated that different motor imagery tasks (imagined index finger abduction, power grip, and precision grip) evoked different numbers of corticomotoneuronal (CM) cells [46]. If different corticospinal excitability are activated by the motor imagery tasks, then different numbers of CM cells may be recruited during the performance of various tasks.

E. Limitations and Future Work

In the present BCI system, we used the same nine EEG channels for each subject. Previous studies noted that the selection of channels for individual subjects is necessary to avoid recording redundant information from the channels [47], [48]. The exact selection of EEG channels that record the ERD should be different across subjects due to different head shapes [49]. Hence, a helpful approach would be to identify the exact channels for each subject to obtain the best record of ERD strength. In the future, we will investigate whether a specific set of EEG channels is effective for each subject. A study revealed that different ERD strengths are positively related to corticospinal excitability [24]. This conclusion inspired us to test the relationship between ERD strength and corticocortical contributions to imagined grasping in our future research. We set the ERD frequency band at 8-20 Hz, as this frequency was proposed in a previous paper [50]. ERD strength varies slightly between subjects in the most reactive frequency bands [51]. The specific frequency band that should be used in our system remains to be determined.

In the current study, we aimed to make a greater contribution to society. Recently, proposed BCI systems have been applied to rehabilitate poststroke hemiparesis [52], [53], and we would like to subsequently apply our system in the rehabilitation of stroke patients.

V. Conclusion

In this study, we performed Experiment 1 to explore the differences in MEPs between imagined power grip and resting conditions. Experiment 2 explored the neural mechanism of 3 different imagined hand motor tasks in the brain. Both experiments were performed using a motor imagery-based BCI system. Our results reveal that later synapses were recruited in an imagined power grip, consistent with the neural mechanism in voluntary movements. In addition, we performed an adjusted experiment to avoid the effect of MEP size. We also note that corticospinal excitability is higher in imagined precision grip and index finger abduction. Our findings will contribute substantially to solving the problem of different hand movements in BCI control and illustrate that ERD is useful as a biomarker in BCI control once again. Thus, if researchers wish to design BCI control robots or similar devices for controlling hand movement or other fine movements, the synaptic inputs to the brain for different precision hand movements should be considered.

References

[1] J. Decety, M. Jeannerod, M. Germain, and J. Pastene, "Vegetative response during imagined movement is proportional to mental effort," *Behavioural Brain Res.*, vol. 42, no. 1, pp. 1–5, Jan. 1991.
[2] M. Keller, W. Taube, and B. Lauber, "Task-dependent activation of distinct fast and slow(er) motor pathways during motor imagery," *Brain Stimulation*, vol. 11, no. 4, pp. 782–788, Jul. 2018.
[3] A. D. Iacono, K. Ashcroft, and D. Zubac, "Ain't just imagination! effects of motor imagery training on strength and power performance of athletes during detraining," *Med. Sci. Sports Exercise*, vol. 53, no. 11, pp. 2324–2332, 2021.
[4] K. Kilteni, B. J. Andersson, C. Houborg, and H. H. Ehrsson, "Motor imagery involves predicting the sensory consequences of the imagined movement," *Nature Commun.*, vol. 9, no. 1, pp. 1–9, Dec. 2018.
[5] M. Lotze and U. Halsband, "Motor imagery," *J. Physiol. Pairs*, vol. 99, pp. 386–395, Feb. 2006.
[6] M. Jeannerod, "From my self to other selves: A revised framework for the self/other differentiation," in *Sensorimotor Foundations of Higher Cognition*. Oxford, U.K.: Oxford Univ. Press, 2008, pp. 233–248.
[7] J. Grezes and J. Decety, "Functional anatomy of execution, mental simulation, observation, and verb generation of actions: A meta-analysis," *Hum. Brain Mapping*, vol. 12, no. 1, pp. 1–19, Jan. 2001.
[8] M. Jeannerod, "Neural simulation of action: A unifying mechanism for motor cognition," *NeuroImage*, vol. 14, no. 1, pp. S103–S109, Jul. 2001.
[9] P. Federico and M. A. Perez, "Distinct corticocortical contributions to human precision and power grip," *Cerebral Cortex*, vol. 27, no. 11, pp. 5070–5082, Nov. 2017.
[10] M. Takemi, T. Maeda, Y. Masakado, H. R. Siebner, and J. Ushiba, "Muscle-selective disinhibition of corticomotor representations using a motor imagery-based brain-computer interface," *NeuroImage*, vol. 183, pp. 597–605, Dec. 2018.
[11] X. Zhang, H. Li, T. Xie, Y. Liu, J. Chen, and J. Long, "Movement speed effects on beta-band oscillations in sensorimotor cortex during voluntary activity," *J. Neurophysiol.*, vol. 124, no. 2, pp. 352–359, Aug. 2020.
[12] P. Zhuang, C. Toro, J. Grafman, P. Manganotti, L. Leocani, and M. Hallett, "Event-related desynchronization (ERD) in the alpha frequency during development of implicit and explicit learning," *Electroencephalogr. Clin. Neurophysiol.*, vol. 102, no. 4, pp. 374–381, Apr. 1997.
[13] M. Song and J. Kim, "A paradigm to enhance motor imagery using rubber hand illusion induced by visuo-tactile stimulus," *IEEE Trans. Neural Syst. Rehabil. Eng.*, vol. 27, no. 3, pp. 477–486, Mar. 2019.
[14] I. Daly, C. Blanchard, and N. P. Holmes, "Cortical excitability correlates with the event-related desynchronization during brain–computer interface control," *J. Neural Eng.*, vol. 15, no. 2, Apr. 2018, Art. no. 026022.

[15] N. A. Grigorev et al., "A BCI-based vibrotactile neurofeedback training improves motor cortical excitability during motor imagery," *IEEE Trans. Neural Syst. Rehabil. Eng.*, vol. 29, pp. 1583–1592, 2021.

[16] V. Dietz, "Neural coordination of bilateral power and precision finger movements," *Eur. J. Neurosci.*, vol. 54, no. 12, pp. 8249–8255, Dec. 2021.

[17] Y. Suzuki et al., "Evidence that brain-controlled functional electrical stimulation could elicit targeted corticospinal facilitation of hand muscles in healthy young adults," *Neuromodulation, Technol. Neural Interface*, Jan. 2022.

[18] J. Boonzaier, P. I. Petrov, W. M. Otte, N. Smirnov, S. F. W. Neggers, and R. M. Dijkhuizen, "Design and evaluation of a rodent-specific transcranial magnetic stimulation coil: An in silico and in vivo validation study," *Neuromodulation, Technol. Neural Interface*, vol. 23, no. 3, pp. 324–334, Apr. 2020.

[19] W. D. Liang, Y. Xu, J. Schmidt, L. X. Zhang, and K. L. Ruddy, "Upregulating excitability of corticospinal pathways in stroke patients using TMS neurofeedback; a pilot study," *NeuroImage, Clin.*, vol. 28, Jan. 2020, Art. no. 102465.

[20] G. Pouchelon et al., "The organization and development of cortical interneuron presynaptic circuits are area specific," *Cell Rep.*, vol. 37, no. 6, Nov. 2021, Art. no. 109993.

[21] K. Takasaki et al., "Targeted up-conditioning of contralesional corticospinal pathways promotes motor recovery in poststroke patients with severe chronic hemiplegia," in *Brain-Computer Interface Research*. Cham, Switzerland: Springer, 2019, pp. 75–82.

[22] J. Höhne, E. Holz, P. Staiger-Sälzer, K.-R. Müller, A. Kübler, and M. Tangermann, "Motor imagery for severely motor-impaired patients: Evidence for brain-computer interfacing as superior control solution," *PLoS ONE*, vol. 9, no. 8, Aug. 2014, Art. no. e104854.

[23] T. Aflalo et al., "Decoding motor imagery from the posterior parietal cortex of a tetraplegic human," *Science*, vol. 348, no. 6237, pp. 906–910, 2015.

[24] G. Pfurtscheller and F. H. L. da Silva, "Event-related EEG/MEG synchronization and desynchronization: Basic principles," *Clin. Neurophysiol.*, vol. 110, pp. 1842–1857, Nov. 1999.

[25] M. Niquille et al., "Neurogliaform cortical interneurons derive from cells in the preoptic area," *eLife*, vol. 7, Mar. 2018, Art. no. e32017.

[26] J. Cirillo, J. G. Semmler, R. A. Mooney, and W. D. Byblow, "Primary motor cortex function and motor skill acquisition: Insights from threshold-hunting TMS," *Exp. Brain Res.*, vol. 238, nos. 7–8, pp. 1745–1757, Aug. 2020.

[27] T. Zandonai, F. Pizzolato, E. Tam, P. Bruseghini, C. Chiamulera, and P. Cesari, "The effects of nicotine on cortical excitability after exercise: A double-blind randomized, placebo-controlled, crossover study," *J. Clin. Psychopharmacol.*, vol. 40, no. 5, pp. 495–498, 2020.

[28] A. Guerra et al., "Detecting cortical circuits resonant to high-frequency oscillations in the human primary motor cortex: A TMS-tACS study," *Sci. Rep.*, vol. 10, no. 1, pp. 1–11, May 2020.

[29] I. Daly, C. Blanchard, and N. P. Holmes, "Cortical excitability correlates with the event-related desynchronization during brain–computer interface control," *J. Neural Eng.*, vol. 15, no. 2, Apr. 2018, Art. no. 026022.

[30] M. Mukaino et al., "Efficacy of brain-computer interface-driven neuromuscular electrical stimulation for chronic paresis after stroke," *J. Rehabil. Med.*, vol. 46, no. 4, pp. 378–382, 2014.

[31] B. A. Murphy, J. P. Miller, K. Gunalan, and A. B. Ajiboye, "Contributions of subsurface cortical modulations to discrimination of executed and imagined grasp forces through stereoelectroencephalography," *PLoS ONE*, vol. 11, no. 3, Mar. 2016, Art. no. e0150359.

[32] T. Ono et al., "Brain-computer interface with somatosensory feedback improves functional recovery from severe hemiplegia due to chronic stroke," *Frontiers Neuroeng.*, vol. 7, p. 19, Jul. 2014.

[33] R. Bauer, M. Fels, M. Vukelić, U. Ziemann, and A. Gharabaghi, "Bridging the gap between motor imagery and motor execution with a brain–robot interface," *NeuroImage*, vol. 108, pp. 319–327, Mar. 2015.

[34] R. M. Hardwick, S. Caspers, S. B. Eickhoff, and S. P. Swinnen, "Neural correlates of action: Comparing meta-analyses of imagery, observation, and execution," *Neurosci. Biobehav. Rev.*, vol. 94, pp. 31–44, Nov. 2018.

[35] K. Kilteni, B. J. Andersson, C. Houborg, and H. H. Ehrsson, "Motor imagery involves predicting the sensory consequences of the imagined movement," *Nature Commun.*, vol. 9, no. 1, pp. 1–9, Dec. 2018.

[36] P. Federico and M. A. Perez, "Distinct corticocortical contributions to human precision and power grip," *Cerebral Cortex*, vol. 27, no. 11, pp. 5070–5082, Nov. 2017.

[37] V. Di Lazzaro and U. Ziemann, "The contribution of transcranial magnetic stimulation in the functional evaluation of microcircuits in human motor cortex," *Frontiers Neural Circuits*, vol. 7, p. 18, Feb. 2013.

[38] V. D. Lazzaro et al., "The effect on corticospinal volleys of reversing the direction of current induced in the motor cortex by transcranial magnetic stimulation," *Exp. Brain Res.*, vol. 138, no. 2, pp. 268–273, May 2001.

[39] V. D. Lazzaro et al., "I-wave origin and modulation," *Brain Stimulation*, vol. 5, no. 4, pp. 512–525, Oct. 2012.

[40] M. Hamada, N. Murase, A. Hasan, M. Balaratnam, and J. C. Rothwell, "The role of interneuron networks in driving human motor cortical plasticity," *Cerebral Cortex*, vol. 23, no. 7, pp. 1593–1605, 2013.

[41] M. Hamada, J. M. Galea, V. D. Lazzaro, P. Mazzone, U. Ziemann, and J. C. Rothwell, "Two distinct interneuron circuits in human motor cortex are linked to different subsets of physiological and behavioral plasticity," *J. Neurosci.*, vol. 34, no. 38, pp. 12837–12849, Sep. 2014.

[42] R. Hanajima et al., "Mechanisms of intracortical I-wave facilitation elicited with paired-pulse magnetic stimulation in humans," *J. Physiol.*, vol. 538, no. 1, pp. 253–261, Jan. 2002.

[43] M. Hamada, N. Murase, A. Hasan, M. Balaratnam, and J. C. Rothwell, "The role of interneuron networks in driving human motor cortical plasticity," *Cereb. Cortex*, vol. 23, no. 7, pp. 1593–1605, 2013.

[44] M. Hamada, J. M. Galea, V. Di Lazzaro, P. Mazzone, U. Ziemann, and J. C. Rothwell, "Two distinct interneuron circuits in human motor cortex are linked to different subsets of physiological and behavioral plasticity," *J. Neurosci.*, vol. 34, no. 38, pp. 12837–12849, Sep. 2014.

[45] R. B. Muir and R. N. Lemon, "Corticospinal neurons with a special role in precision grip," *Brain Res.*, vol. 261, no. 2, pp. 312–316, Feb. 1983.

[46] S. Yahagi and T. Kasai, "Facilitation of motor evoked potentials (MEPs) in first dorsal interosseous (FDI) muscle is dependent on different motor images," *Electroencephalogr. Clin. Neurophysiol./Electromyography Motor Control*, vol. 109, no. 5, pp. 409–417, Oct. 1998.

[47] J. Jin, Y. Miao, I. Daly, C. Zuo, D. Hu, and A. Cichocki, "Correlation-based channel selection and regularized feature optimization for MI-based BCI," *Neural Netw.*, vol. 118, pp. 262–270, Oct. 2019.

[48] X. Ma, S. Qiu, W. Wei, S. Wang, and H. He, "Deep channel-correlation network for motor imagery decoding from the same limb," *IEEE Trans. Neural Syst. Rehabil. Eng.*, vol. 28, no. 1, pp. 297–306, Jan. 2020.

[49] G. Pfurtscheller, C. Brunner, A. Schlögl, and F. H. L. da Silva, "Mu rhythm (de) synchronization and EEG single-trial classification of different motor imagery tasks," *Neuroimage*, vol. 31, no. 1, pp. 153–159, May 2006.

[50] C. Neuper, G. Müller-Putz, R. Scherer, and G. Pfurtscheller, "Motor imagery and EEG-based control of spelling devices and neuroprostheses," *Prog. Brain Res.*, vol. 159, no. 10, pp. 393–409, 2006.

[51] G. Pfurtscheller, C. Brunner, A. Schlögl, and F. H. L. da Silva, "Mu rhythm (de) synchronization and EEG single-trial classification of different motor imagery tasks," *NeuroImage*, vol. 31, no. 1, pp. 153–159, 2006.

[52] Z. Qiu, S. Chen, I. Daly, J. Jia, X. Wang, and J. Jin, "BCI-based strategies on stroke rehabilitation with avatar and FES feedback," 2018, *arXiv:1805.04986*.

[53] I. Kuzovkin, K. Tretyakov, A. Uusberg, and R. Vicente, "Mental state space visualization for interactive modeling of personalized BCI control strategies," *J. Neural Eng.*, vol. 17, no. 1, Feb. 2020, Art. no. 016059.